

Globular Cluster Formation at High Density: A model for Elemental Enrichment with Fast Recycling of Massive-Star Debris

Bruce G. Elmegreen¹

ABSTRACT

The self-enrichment of massive star clusters by p-processed elements is shown to increase significantly with increasing gas density as a result of enhanced star formation rates and stellar scatterings compared to the lifetime of a massive star. Considering the type of cloud core where a globular cluster might have formed, we follow the evolution and enrichment of the gas and the time dependence of stellar mass. A key assumption is that interactions between massive stars are important at high density, including interactions between massive stars and massive star binaries that can shred stellar envelopes. Massive-star interactions should also scatter low-mass stars out of the cluster. Reasonable agreement with the observations is obtained for a cloud core mass of $\sim 4 \times 10^6 M_\odot$ and a density of $\sim 2 \times 10^6 \text{ cm}^{-3}$. The results depend primarily on a few dimensionless parameters, including, most importantly, the ratio of the gas consumption time to the lifetime of a massive star, which has to be low, $\sim 10\%$, and the efficiency of scattering low-mass stars per unit dynamical time, which has to be relatively large, such as a few percent. Also for these conditions, the velocity dispersions of embedded globular clusters should be comparable to the high gas dispersions of galaxies at that time, so that stellar ejection by multi-star interactions could cause low-mass stars to leave a dwarf galaxy host altogether. This could solve the problem of missing first-generation stars in the halos of Fornax and WLM.

Subject headings: Galaxies: star clusters — Galaxies: star formation — globular clusters: general

1. Introduction

Most globular clusters (GCs) in the Milky Way have two populations of stars in approximately equal proportion with a first generation (G1) relatively abundant in Oxygen

¹IBM Research Division, T.J. Watson Research Center, 1101 Kitchawan Road, Yorktown Heights, NY 10598; bge@us.ibm.com

compared to Sodium and a second generation (G2) the reverse. This bimodality is presumably the result of contamination of the G2 stars by the products of p-process nucleosynthesis in the G1 stars, particularly the reactions ^{22}Ne to ^{23}Na along with the simultaneous destruction of ^{16}O at a temperature of 2×10^7 K (Denissenkov & Denissenkova 1990; Decressin et al. 2007a). Other elemental anti-correlations include Mg with Al (e.g., Carretta et al. 2014), explained by Langer et al. (1993) and others as a result of high temperature ($T > 7 \times 10^7$ K) proton-capture plus beta-decay that transforms ^{24}Mg into ^{25}Mg , ^{26}Mg and ^{27}Al . Also in some GCs, stellar Nitrogen anti-correlates with Carbon and Oxygen (Dickens et al. 1991), with a total C+N+O abundance that is about constant, suggesting a CNO cycle. Reviews of these abundance anomalies are in Gratton et al. (2004), Charbonnel (2005), Gratton et al. (2012), Renzini et al. (2015), and Bastian (2015).

Light element anomalies from the CNO cycle and the NeNa- and MgAl-chains are peculiar to the GCs and are not in field or halo stars (Gratton et al. 2000; Charbonnel 2005; Prantzos & Charbonnel 2006). Because they involve high-temperature reactions and the stars in which they are observed today are too low in mass to have had such p-process reactions themselves (Gratton et al. 2001), the Na-excess and Al-excess stars in current GCs had to form in gas that was pre-enriched with these elements (Cottrell & Da Costa 1981), most likely from the previous generation of stars as mentioned above. The debris from this previous generation may also have mixed with some left-over initial gas to explain an anticorrelation between Li, which is destroyed in stars, and Na, which is produced (Pasquini et al. 2005; Bonifacio et al. 2007; Decressin et al. 2007a), and to explain the difference between the high enrichment in the nuclear burning regions of massive stars and the observed enrichment in low mass stars (Decressin et al. 2007b, table 4).

The first generation has been proposed to include normal massive stars (Cottrell & Da Costa 1981), such as rapidly spinning massive stars (Prantzos & Charbonnel 2006), which, because of their rotation, bring p-processed material from the H-burning zone into the envelope and then shed it along the equator via centrifugal force and radiation pressure (Prantzos & Charbonnel 2006; Decressin et al. 2007b). Binary massive stars with Roche lobe overflow are also an option (de Mink et al. 2009). AGB stars (D’Ercole et al. 2008) shed processed gas at low speed too and may be a source of the anomalies, although the near-constant C+N+O does not look like a byproduct of AGB stars, which make carbon during Helium burning (Charbonnel 2005); NGC 1851 may be an exception though (Yong et al. 2014; Simpson et al. 2017). Renzini et al. (2015) discuss ways in which the AGB option might still be viable. Other models for the bimodality include proto-stellar disk accretion (Bastian et al. 2013a), supermassive stars (Denissenkov & Hartwick 2014; Denissenkov et al. 2015), GC-merging in dwarf galaxy hosts (Bekki & Tsujimoto 2016), and AGB wind re-collection in the pressurized cavity around the GC (D’Ercole et al. 2016).

A problem with these models is that the stellar debris is only a small fraction of the total stellar mass in a normal IMF. This implies that because the current G1 and G2 masses are comparable to each other, the mass in the original G1 population had to be at least the inverse of this fraction times the current G1 mass. For the model with rapidly rotating massive stars and a normal IMF, the original cluster had to be ~ 20 times the current G1 mass (Decressin et al. 2007b), and for the AGB model, the original cluster had to be > 10 times the current mass (D’Ercole et al. 2008). The missing 90%-95% of the G1 stars had to escape, and even more had to escape if G2 stars escaped too, which is likely. These escaping stars presumably comprise the halo of the Milky Way (Prantzos & Charbonnel 2006; Martell, et al. 2011), but such large halo amounts are not evident in the Fornax or WLM dwarf galaxies (Larsen et al. 2012, 2014; Elmegreen et al. 2012).

Another constraint on the models is that there is virtually no elemental contamination from G1 supernova inside the G2 stars (Charbonnel 2005; Renzini 2013). In the model with rapidly rotating massive stars, this constraint implies that the G2 stars formed quickly, before the G1 supernovae exploded. A potential problem here is that without supernovae, the gas that formed G1 may not be cleared away from a massive cluster (Ginsburg et al. 2016; Lin et al. 2016), causing a high fraction of it to turn into stars. Such high efficiency prevents the cluster from shedding its excess G1 stars during rapid gas loss (Krause et al. 2016), and then the final cluster is too massive and it has too many G1 stars compared to G2. Cluster clearing was tested by Bastian et al. (2014b), who found that clusters with masses up to $10^6 M_{\odot}$ and ages between 20 and 30 Myr are often clear of gas. This age is old enough for some supernovae to have occurred. Without gas, star formation stops and a prolonged epoch of secondary star formation that feeds on G1 debris does not occur.

Secondary or delayed star formation as in the AGB model is also not observed in today’s massive clusters at the predicted age range of 10-1000 Myr (Bastian et al. 2013b; Cabrera-Ziri et al. 2014), although it was reported by Li et al. (2016) whose result was then questioned by Cabrera-Ziri et al. (2016). Neither do massive 100 Myr old clusters have obvious gas from accumulated winds or secondary accretion (Bastian & Strader 2014).

Here we investigate further the model by Prantzos & Charbonnel (2006) and others, where p-process contamination from massive stars is quickly injected into a star-forming cloud core and incorporated into other forming stars. We consider conditions appropriate for the early Universe where the interstellar pressure was much higher than it is today. This pressure follows from the observation that star formation was ~ 10 times more active per unit area than it is now (Genzel et al. 2010) as a result of a factor of ~ 10 higher gas column density (Tacconi et al. 2010; Daddi et al. 2010). Because interstellar pressure scales with the square of the column density ($P \sim G\Sigma^2$), the pressure was $\sim 100\times$ larger when GCs

formed than it is in typical star-forming regions today. Consequently, the core of the GC-forming cloud was likely to have a higher density and therefore a larger number of free-fall times, such as 10 or more, before the first supernovae occurred. Star formation could have occurred so quickly and the energy dissipation rate at high density could have been so high that feedback from massive stars had little effect on cloud dispersal before the supernova era (e.g., Wunsch et al. 2015). Also at high density, massive stars experience a significant drag force from gas and low-mass stars (Ostriker 1999), causing them to spiral into an even more compact configuration. High stellar densities lead to the dispersal of extrusion disks filled with stellar envelope material (Prantzos & Charbonnel 2006), and also to close encounters between massive stars or between tight massive binaries and massive stars, which can shred the stellar envelopes (Gaburov et al. 2010). High stellar densities may also make supermassive stars by coalescence (Ebisuzaki et al. 2001; Bally & Zinnecker 2005), and these stars can produce the highest-temperature p-process elements (Denissenkov et al. 2015).

A related point is that at high density, a significant fraction of early-forming low-mass stars should have been ejected from the cloud core by interactions with massive binaries and massive multi-body collisional systems. This could occur long before “infant mortality,” when the final clearing of gas signals the end of the star formation process. Rapid and continuous stellar ejections by massive star interactions are well observed in numerical simulations of cluster formation (Reipurth & Clarke 2001; Bate & Bonnell 2005; Fujii & Portegies Zwart 2013). Because massive three-body collisions can also dump nearly a supernova’s worth of kinetic energy into a region (Gaburov et al. 2010; Umbreit et al. 2008), the gas in the core should be continuously agitated. The corresponding changes in the gravitational potential energy of the gas should eject even more low-mass stars, in analogy to the proposed ejection of stars and dark matter from the cores of young star-bursting dwarf galaxies (Governato et al. 2012; El-Badry et al. 2016).

Dense cores are likely to continue accreting from the cloud envelope for many core dynamical times. If the core plus envelope gas mixes with stellar debris and forms new stars, then a succession of stellar populations will occur with ever-increasing levels of p-process elements. By the time the first massive stars begin to supernova and clear away the gas, some 3-7 Myr after star formation begins (Heger et al. 2003), there should be a wide range of p-process elements in the stars that have formed. The model presented below shows that this range can reproduce the observations for certain values of dimensionless parameters.

A key observation is that elemental enrichment in GCs seems to be discrete (Marino et al. 2011; Carretta et al. 2012, 2014; Renzini et al. 2015). Discreteness requires burst-like contamination, and in the stellar interaction model here, that means intermittent events of catastrophic massive-star interactions. The interactions occur where the density is high-

est, so either the stellar density in the cloud core varies episodically with a burst of stellar collisions following each high-density phase, or there are several mass-segregated cores in a proto-GC (McMillan et al. 2007; Fujii & Portegies Zwart 2013) and each has its own burst of intense interactions. Both situations are likely and could contribute to discrete populations of stars. The temporal density variations would presumably follow from the time-changing gravitational potential in the cluster core, as stellar envelope mass is disbursed along with cloud mass through collisions, and then recollected in the core after a dynamical time because of self-gravity and background pressure.

The following sections examine this model in more detail. Section 2.1 outlines the basic model of GC formation at high density, section 2.2 presents the equations that govern this model, giving some analytical solutions in section 2.3, and section 3 shows the results. A conclusion that highlights the main assumptions of the model and their implications for high-density cluster formation is in Section 4.

2. Star Formation in Stellar Debris

2.1. Basic Model

The basic scale of GC formation considered here involves a molecular cloud core of mass $\sim 4 \times 10^6 M_\odot$ in a spherical region of radius ~ 3 pc. A larger region of lower-density gas should surround this core, possibly in the form of filaments or spokes which continuously deliver new gas (Klessen et al. 1998; Myers 2009). Perhaps the total mass involved with the proto-GC and its neighborhood is $\sim 10^7 M_\odot$ or more, as observed for a massive dense region in the Antenna galaxy (Herrera et al. 2012; Johnson et al. 2015). The core molecular density for the above numbers is $2.2 \times 10^6 \text{ cm}^{-3}$ and the free fall time ($= (3\pi/32G\rho)^{0.5}$) is 0.03 Myr. The ratio of the core mass to the free fall time, $133 M_\odot \text{ yr}^{-1}$, is a measure of the core accretion rate during core formation. If this core collapsed from the interstellar gas at the typical rate of σ_{ISM}^3/G for interstellar velocity dispersion σ_{ISM} , then $\sigma_{\text{ISM}} = 82 \text{ km s}^{-1}$, which is not unusual for high-redshift disk galaxies (e.g., Förster Schreiber, et al. 2009). The accretion rate of low-density peripheral gas on to the core should be much less than the initial core formation rate.

The fiducial cloud core mass of $\sim 4 \times 10^6 M_\odot$ was chosen to produce a final GC mass of around $2 \times 10^5 M_\odot$, which is at the peak of the GC mass distribution function (Harris & Racine 1979). The first factor of ~ 10 in mass reduction follows from our model including multiple generations of star formation in the core and mass loss from stellar ejection, as required by the observed spread in p-processed elemental abundance. Another

factor of ~ 2 reduction in the GC mass is likely from evaporation over a Hubble time (McLaughlin & Fall 2008).

The average core surface density in this basic model, $1.4 \times 10^5 M_\odot \text{pc}^{-2}$, is comparable to the maximum for stellar systems (Hopkins et al. 2010; Walker et al. 2016). The core velocity dispersion is $\sim 76 \text{ km s}^{-1}$, which is a factor of 2 higher than for massive clusters today, but not unreasonable for a young galaxy where the gas turbulence speed is this high. Over time, the cluster should expand and the dispersion decrease (e.g. Gieles & Renaud 2016). The original cluster dispersion is high enough to make feedback-driven gas loss difficult before the supernova era (Matzner & Jumper 2015; Krause et al. 2016). We consider that because of this difficulty, the efficiency of star formation per unit free-fall time might be relatively high, $\sim 10\%$, instead of the usual 1% (Krumholz & Tan 2007). Then the gas consumption time, which is the free-fall time divided by the efficiency, is 0.3 Myr. The significant point here is that this consumption time is much less than the evolution time of a high-mass star.

One potential implication of the high velocity dispersion in GC-forming cloud cores is that stars ejected by time-changing gravitational potentials (e.g., binary or multi-star interactions and the induced rapid gas motions) should also have fairly high velocities. Dynamical ejection processes can be much more energetic than thermal evaporation from a random walk. This offers an intriguing solution to the problem stated in the introduction that Fornax and WLM do not have stellar halos massive enough to include all of the required mass of G1 stars that should have been ejected from their GCs. In fact these are dwarf galaxies with very slow internal motions: the Fornax dwarf spheroidal galaxy has a $\sim 12 \text{ km s}^{-1}$ internal velocity dispersion and a much lower rotation speed (Walker et al. 2006), while WLM has a 36 km s^{-1} rotation speed (Leaman et al. 2012). Stars that are ejected at a factor of 1.5 to 2 times the escape speed of the GC could leave the galaxy. This possibility leads to the prediction that *galaxies with slow internal motions should have a systematic depletion in halo stars from the G1 population that escaped their GCs*. A similar conclusion was reached by Khalaj & Baumgardt (2016) based on stellar loss from GCs during gas expulsion.

The IMF for all star formation is assumed to be fully populated and given by the log-normal distribution in Paresce & De Marchi (2000) for stellar mass $0.1 M_\odot < M < 0.8 M_\odot$, with mass at the peak $M_C = 0.33 M_\odot$ and dispersion $\sigma = 0.34 M_\odot$, and by a power law with the Salpeter slope -2.35 above $0.8 M_\odot$ (see also Prantzos & Charbonnel 2006). The upper limit to the stellar mass will be varied from $M_{\text{upper}} = 100 M_\odot$ to $300 M_\odot$, with the high value considered because of stellar coalescence. Note that a $320 M_\odot$ star has been suggested for the dense massive cluster R136 in the LMC (Crowther et al. 2010; Crowther et al. 2016), and stars more massive than $100 M_\odot$ were found in the dense cluster in NGC 5253 (Smith et al. 2016). Stars with masses larger than $20 M_\odot$ are assumed to make p-

process elements (Decressin et al. 2007a) and mix them into their stellar envelopes, which are defined to be all of the stellar mass outside of the He core, as given by Prantzos & Charbonnel (2006). For $M_{\text{upper}} = 100 M_{\odot}$, the fraction of the total stellar mass in the form of these envelopes is $f_{\text{env}} = 7.9\%$, which is the product of the fraction of the IMF in stars with $M > 20 M_{\odot}$ (12.1%) and the average fraction of this stellar mass in the form of envelopes (65.1%). For $M_{\text{upper}} = 300 M_{\odot}$, $f_{\text{env}} = 9.3\%$ (16.4% of the IMF is in $M > 20 M_{\odot}$ stars and 56.8% of that mass is in envelopes). Also for these two upper masses, the fraction of the total stellar mass in long-lived, low-mass stars ($M < 0.8 M_{\odot}$), is $f_{\text{LM}} = 31.2\%$ and 29.7%, respectively. The formation of p-process elements and the delivery of these elements into the stellar envelopes and equatorial disks is assumed to proceed at a steady rate with an average timescale $t_{\text{evol}} = 3$ Myr, the lifetime of a high-mass star.

Regarding the contamination by p-processed elements, we note that the [O/Na] ratio in GCs varies from the large value of ~ 0.4 in G1 to the small value of ~ -1.4 in G2, depending on the GC (-1.4 is for NGC 2802; Carretta 2006; Prantzos & Charbonnel 2006; Gratton et al. 2012). The maximum value is about the same as in field stars and the minimum value is close what is expected in the envelope of a massive star near the end of its pre-main sequence phase (Prantzos & Charbonnel 2006). The range of observed values, 1.8 dex, is less than the change expected inside the nuclear burning regions of massive stars, which is 2.8 to 3.4 dex (depending on reaction rates) in Decressin et al. (2007a). This difference allows for some dilution of the core region with the envelope of the star before dispersal. The full range in today’s stars therefore extends from the presumed initial condition when the first generation formed, to a value that represents the near-complete conversion of a massive stellar envelope into one or more G2 stars. Values of [O/Na] between these extremes correspond to some combination of incomplete mixing of the processed debris with first generation gas, and partially processed gas from stars that have not yet finished their main sequence evolution (Scenarios II and I in Prantzos & Charbonnel 2006).

The dilution proportions of processed stellar envelope gas and original cloud gas has also been estimated from the relative Li abundance in the G2 stars, considering that Li will be destroyed in the massive G1 stars. The observations suggest that up to 70% of the mass of a G2 star could come from the debris of G1 stars (Decressin et al. 2007b). This high fraction limits the amount of accretion from the cloud envelope during the star formation process.

As mentioned above, the enriched gas is assumed to come from stellar equatorial disks (Prantzos & Charbonnel 2006) and stellar debris generated by close interactions. For example, Gaburov et al. (2010) show that massive binaries that collide with another star can merge and puff up (see also Fregeau et al. 2004), and that continued collisions with the

third star before merging can shred the common envelope. Mass loss fractions of $\sim 10\%$ are feasible in this situation. Umbreit et al. (2008) also consider the implications of collisions and suggest that the kinetic energy from collision-induced mass loss can clear gas away every few million years from aging globular clusters. This kinetic energy is comparable to that of a supernova (Gaburov et al. 2010). For the dense cloud cores considered here, that is not enough energy to clear away the gas, which is highly dissipative, but it could be enough for later stages of cluster formation after a significant amount of gas has turned into stars, and that is also when the supernovae themselves begin to clear the clusters of residual gas. We assume here that all of the stellar debris, i.e., from massive-star equatorial disks (Prantzos & Charbonnel 2006), massive star collisions, and Roche lobe overflow around massive binaries (de Mink et al. 2009), brings p-processed material from the envelopes of massive stars into the dense cloud core where it mixes with existing and newly accreted core gas on the turbulent crossing time (~ 0.1 Myr), and is incorporated into new stars. This process continues for ~ 3 Myr, forming the whole final cluster, at which point supernovae begin to remove the remaining gas.

2.2. Model Equations

Consistent with these assumptions, we consider an initial cloud core of mass $M_{\text{gas}}(t = 0)$ in which stars begin to form, and a continuous accretion of new cloud gas onto this core at a rate R_{acc} . Stars are assumed to form in the core with a constant consumption time, t_{consume} (equal to t_{ff} divided by the efficiency per free fall time). The effect of varying the consumption time will be discussed below. The formation rates of low ($< 0.8 M_{\odot}$), intermediate ($0.8 M_{\odot} - 20 M_{\odot}$) and high ($> 20 M_{\odot}$) mass stars are given by the star formation rate in the core multiplied by the fractions of the IMF in these three mass intervals:

$$dM_{\text{star,LM}}/dt = f_{\text{LM}}M_{\text{gas}}(t)/t_{\text{consume}} \quad (1)$$

$$dM_{\text{star,IM}}/dt = f_{\text{IM}}M_{\text{gas}}(t)/t_{\text{consume}} \quad (2)$$

$$dM_{\text{star,HM}}/dt = f_{\text{HM}}M_{\text{gas}}(t)/t_{\text{consume}}, \quad (3)$$

where $f_{\text{LM}} = 0.312$, $f_{\text{IM}} = 0.567$, and $f_{\text{HM}} = 0.121$ for an IMF with a most massive star of $100 M_{\odot}$, and where $f_{\text{LM}} = 0.297$, $f_{\text{IM}} = 0.540$, and $f_{\text{HM}} = 0.164$ for an IMF with a most massive star of $300 M_{\odot}$ (Sect. 2.1). The total mass formed in these stars is

$$M_{\text{star,LM}}(t) = \int_0^t \dot{M}_{\text{star,LM}} dt, \dots \quad (4)$$

and so on for the other mass ranges. Here we use the notation $\dot{M} = dM/dt$. The total mass for all stars is $M_{\text{star}} = M_{\text{star,LM}} + M_{\text{star,IM}} + M_{\text{star,HM}}$.

For the gas, we track the primordial and enriched gas masses separately. The primordial gas is a combination of what was originally in the cloud core plus what gets accreted after star formation begins, and it also includes the part of the stellar envelope debris that was not converted into p-processed elements. We assume that massive stars make p-process elements continuously and that mixing from rapid rotation puts these elements into the stellar envelopes continuously. Thus we conceptually divide the envelope mass into an unprocessed fraction at the original primordial abundance, and a completely processed, or enriched, fraction at the abundance of fully processed material. The total envelope is a combination of these, giving a partially-processed elemental abundance that comes from the dilution of fully processed material by the mass that is still in an unprocessed form.

With these assumptions, the rate of change of the primordial (1st generation) gas mass in the cloud core, $\dot{M}_{\text{gas},1}$, is the increase from stellar debris and envelope accretion minus what goes into stars,

$$\begin{aligned} \dot{M}_{\text{gas},1}(t) = \int_0^t \left(\frac{f_{\text{debr}} \dot{M}_{\text{star,HM}}(t')}{t_{\text{evol}}} \right) (1 - f_{\text{p}}(t')) \left[1 - \frac{t - t'}{t_{\text{evol}}} \right] dt' \\ + R_{\text{acc}}(t) - (1 - f_{\text{p}}(t)) \dot{M}_{\text{star}}(t). \end{aligned} \quad (5)$$

The first term in the integral is from ejection of stellar debris (equatorial disks, collisional debris, Roche-lobe overflow). The term f_{debr} is the average fraction of the mass of a high-mass star that is in the envelope and can be ejected. It equals 0.651 for $M_{\text{upper}} = 100 M_{\odot}$ and 0.568 for $M_{\text{upper}} = 300 M_{\odot}$ (Prantzos & Charbonnel 2006). Division by t_{evol} indicates that we assume this debris is ejected steadily over the evolution time of the massive star, nominally assumed to be $t_{\text{evol}} = 3$ Myr. The quantity $f_{\text{p}}(t')$ is the processed fraction in the gas at time t' , and therefore also the processed fraction in stars that form at time t' , assuming rapid mixing. Thus, $1 - f_{\text{p}}(t')$ is the unprocessed fraction of the mass of the star that previously formed at t' . The last term, $1 - ([t - t']/t_{\text{evol}})$, tracks the remaining unprocessed fraction in the stellar envelope as the concentration of processed material increases linearly with time. This linear increase assumes the p-process elements from the stellar core mix into the stellar envelope at a steady rate. In addition to the integral that represents debris output, the unprocessed gas mass also increases by accretion at the rate R_{acc} . From these additions we subtract the unprocessed gas mass in the cloud core that goes into stars.

The rate of change of processed gas mass in the cloud core, $\dot{M}_{\text{gas},2}$ (2nd generation), is from the addition of stellar debris minus what goes into stars:

$$\dot{M}_{\text{gas},2}(t) = \int_0^t \left(\frac{f_{\text{debr}} \dot{M}_{\text{star,HM}}(t')}{t_{\text{evol}}} \right) (1 - f_{\text{p}}(t')) \left(\frac{t - t'}{t_{\text{evol}}} \right) dt' \quad (6)$$

$$+ \int_0^t \left(\frac{f_{\text{debr}} \dot{M}_{\text{star, HM}}(t')}{t_{\text{evol}}} \right) f_{\text{p}}(t') dt' - f_{\text{p}}(t) \dot{M}_{\text{star}}(t).$$

The first integral represents the originally unprocessed mass fraction in the star when it formed, $(1 - f_{\text{p}}(t'))$, that came out as debris and became more and more contaminated with time (as measured by $[t - t']/t_{\text{evol}}$), and the second integral represents the return of originally processed mass (at fraction f_{p}) into the cloud core. Note that the sum of the processed and unprocessed gas mass rates from equations (5) and (6) equals $\int_0^t [f_{\text{debr}} M_{\text{HM}}(t')/t_{\text{evol}}] dt' + R_{\text{acc}} - dM_{\text{star}}/dt$, which is the total debris rate plus the accretion rate minus the star formation rate.

Now we determine the masses of primordial and enriched gas in the star-forming cloud core by integration,

$$M_{\text{gas},1}(t) = \int_0^t \dot{M}_{\text{gas},1}(t) dt \quad (7)$$

$$M_{\text{gas},2}(t) = \int_0^t \dot{M}_{\text{gas},2}(t) dt, \quad (8)$$

we combine these to get the total gas mass,

$$M_{\text{gas}} = M_{\text{gas},1} + M_{\text{gas},2}, \quad (9)$$

and we determine the mass fractions of enriched gas used above.

$$f_{\text{p}}(t) = \frac{M_{\text{gas},2}}{M_{\text{gas}}}. \quad (10)$$

The low mass stars do not contribute to the above equations except as a long-term sink for stellar mass. However, these stars are important for the observation of GCs today, and this is where stellar ejection and evaporation come in. We assume here that only low and intermediate mass stars leave the cluster by these processes, and we trace only the low mass stellar loss because the intermediate mass stars will have disappeared by now anyway, except as residual collapsed remnants. The high mass stars are assumed to segregate to the center of the GC where essentially all of their p-processes elements are available for gas contamination, as written in the above equations. Thus we need to model the escape of low mass stars.

The discussion in Section 1 suggests that multi-star interactions and gas motions in the GC core occasionally accelerate low mass stars up to escape speed or beyond. Thus the rate of stellar ejection depends on the dynamical rate in the core, and this is directly proportional to both the free-fall rate and the consumption rate in the basic model. This implies that

there is an additional rate of change of the mass of low-mass stars, so equation (1) should be revised to contain an additional term,

$$dM_{\text{star,LM}}/dt = f_{\text{LM}}M_{\text{gas}}(t)/t_{\text{consume}} - f_{\text{eject}}M_{\text{star,LM}}/t_{\text{consume}} \quad (11)$$

for f_{eject} a number less than unity. Recall that $t_{\text{consume}} \sim 10t_{\text{ff}}$, so the ejection time for $f_{\text{eject}} = 0.4$ is 25 free fall times.

2.3. Analytical solution to a dimensionless model

The time dependence of the star formation rate and cloud mass have analytical solutions that are conveniently written using the above equations in dimensionless form. We normalize the gas and stellar masses to the initial cloud core mass, $M_{\text{gas}}(t = 0)$, and the time to the consumption time, t_{consume} , assumed to be constant. Normalized quantities are denoted with a tilde. Then the star formation rate is

$$\frac{d\tilde{M}_{\text{star}}}{d\tilde{t}} = \tilde{M}_{\text{gas}}. \quad (12)$$

The gas mass changes from the addition of stellar debris from high mass stars and cloud envelope accretion and the subtraction of new stars:

$$\frac{d\tilde{M}_{\text{gas}}}{d\tilde{t}} = \frac{f_{\text{debr}}f_{\text{HM}}}{\tilde{t}_{\text{evol}}} \int_0^{\tilde{t}} \frac{\tilde{M}_{\text{star}}(t')}{d\tilde{t}'} dt' + \tilde{R}_{\text{acc}} - \frac{d\tilde{M}_{\text{star}}}{d\tilde{t}}. \quad (13)$$

Here, $\tilde{R}_{\text{acc}} = R_{\text{acc}}t_{\text{consume}}/M_{\text{gas}}(t = 0)$.

Equation (13) can be differentiated with respect to time and equation (12) can be substituted to give a second order linear differential equation,

$$\frac{d^2\tilde{M}_{\text{gas}}}{d\tilde{t}^2} + \frac{d\tilde{M}_{\text{gas}}}{d\tilde{t}} - \gamma\tilde{M}_{\text{gas}} = 0 \quad (14)$$

where

$$\gamma = \frac{f_{\text{debr}}f_{\text{HM}}t_{\text{consume}}}{t_{\text{evol}}} \quad (15)$$

is a dimensionless measure of the relative rate of return of processed gas. For the numbers in the basic model, $\gamma \sim 10^{-2}$. The general solution of equation (15) is the sum of $\tilde{M}_{\text{gas}} \propto \exp(-\alpha\tilde{t})$ with two values of α ,

$$\alpha = 0.5 (1 \pm [1 + 4\gamma]^{0.5}). \quad (16)$$

Using equation (13) again to fit $d\tilde{M}_{\text{gas}}/d\tilde{t}$ at $\tilde{t} = 0$, and defining $\Gamma = (1 + 4\gamma)^{0.5}$, we obtain the solution for normalized gas mass,

$$\tilde{M}_{\text{gas}}(\tilde{t}) = \left(\frac{\Gamma + 0.5 - \tilde{R}_{\text{acc}}}{\Gamma} \right) e^{-0.5(1+\Gamma)\tilde{t}} + \left(\frac{\Gamma - 0.5 + \tilde{R}_{\text{acc}}}{\Gamma} \right) e^{0.5(\Gamma-1)\tilde{t}}. \quad (17)$$

The normalized stellar mass is the time integral over the normalized gas mass, or, ignoring stellar ejection,

$$\tilde{M}_{\text{stars}}(\tilde{t}) = \left(\frac{\Gamma + 0.5 - \tilde{R}_{\text{acc}}}{0.5\Gamma(1 + \Gamma)} \right) \left(1 - e^{-0.5(1+\Gamma)\tilde{t}} \right) + \left(\frac{\Gamma - 0.5 + \tilde{R}_{\text{acc}}}{0.5\Gamma(\Gamma - 1)} \right) \left(e^{0.5(\Gamma-1)\tilde{t}} - 1 \right). \quad (18)$$

This solution consists of an exponentially decaying initial burst of star formation and gas depletion with a timescale approximately equal to the consumption time ($0.5(1 + \Gamma) \sim 1$ in normalized units), followed by a slowly growing gas mass and star formation rate as accretion and stellar debris add to the cloud core (with growth rate $0.5(\Gamma - 1) \sim \gamma \ll 1$).

3. Results

Figure 1 shows numerical solutions to equations (1) to (10) with mass and time normalized as above. The three curves are for different normalized accretion rates, as indicated by their colors and the labels for \tilde{R}_{acc} . The solutions have the parameters discussed above for an IMF extending out to $300 M_{\odot}$, i.e., $f_{\text{HM}} = 0.164$ and $f_{\text{debr}} = 0.568$, and they assume $t_{\text{consume}}/t_{\text{evol}} = 0.1$, which together make $\gamma = 0.0093$. The top left panel shows the cloud core gas mass as a function of time and the top right panel shows the mass of low mass stars without (dashed curves) and with (solid curves) ejection assuming $f_{\text{eject}} = 0.4$. The lower left panel shows the processed fraction in the cloud core, which is also the processed fraction in the stars that form at that time. The analytical solutions to the gas and stellar masses fit exactly on top of the numerical solutions and are not shown in the figure. However, the top left panel has each exponential function from the analytical solution plotted separately as a dotted line; the total solution is the sum of these, as in equation (17).

The lower right panel shows the distribution of the processed fraction, f_{p} , among low-mass stars after star formation is assumed to stop, which is at the time t_{evol} in these models to avoid supernova contamination. All three cases assume stellar ejection with $f_{\text{eject}} = 0.4$. Recall that in observed GCs, f_{p} can range up to 0.7 from the Li abundance (Decressin et al. 2007b), and that is how far the blue histogram goes (which is for $\tilde{R}_{\text{acc}} = 0$). Also from observations, the ratio of stellar mass in the second generation to total stellar mass ranges from ~ 0.5 to ~ 0.8 . For the 3 histograms in Figure 1, the ratios of the masses in all but the

lowest- f_p interval (i.e., the G2 stars) to the sum of all the masses (the G1+G2 stars) is about the same as the observations: 0.63 for the red curve ($\tilde{R}_{\text{acc}} = 0.03$), 0.50 for the green curve ($\tilde{R}_{\text{acc}} = 0.003$) and 0.43 for the blue curve ($\tilde{R}_{\text{acc}} = 0$). The processed fraction f_p increases with time as more and more massive stellar envelopes with their ever-increasing p-process contaminations disperse inside the cloud core (lower left panel). The maximum value of f_p at the end of the star formation time (right-hand limit to the curves in the lower-left panel) increases with decreasing \tilde{R}_{acc} because there is less dilution of the cloud core gas with pristine infall from the cloud envelope.

In equation (11), ejection operates on all low-mass stars regardless of when they form, but it tends to remove a higher proportion of the first stars that form, i.e., weighted toward the G1 stars, than the later stars that form because the first stars have been exposed for the longest time to the multi-star interactions and gas motions that cause ejection. The top right panel of Figure 1 shows that ejection with the assumed $f_{\text{eject}} = 0.4$ reduces the mass in low mass stars by about a factor of 10. Without such stellar loss, the relative proportion of G2 stars shown in the lower right would be much less; i.e., the lowest f_p bin would be much higher compared to the others, although the f_p range in the histogram would be the same.

Related to this age-dependence of stellar ejection is a prediction from this model that the G1 stars should on average be less concentrated in the GC than the G2 stars. This is because the G1 stars have had more opportunities to absorb kinetic energy from multi-stellar interactions in the core than the G2 stars, regardless of whether the stars escape the cluster. Such a central concentration of G2 stars is observed (Gratton et al. 2012).

The left-hand panel of Figure 2 shows the effect of stellar ejection through the parameter f_{eject} on the fraction of the mass in the G2 population. The blue curves assume the usual $t_{\text{consume}}/t_{\text{evol}} = 0.1$ with a range of f_{eject} in equal steps between 0.1 and 0.7. The dashed blue curve with $f_{\text{eject}} = 0.3$ is one of this sequence but it is highlighted to contrast it with the red and green curves, which assume $f_{\text{eject}} = 0.3$ but also $t_{\text{consume}}/t_{\text{evol}} = 0.05$ and 0.2, respectively, for the same value of $\gamma = f_{\text{debr}} f_{\text{HM}} t_{\text{consume}}/t_{\text{evol}}$ (i.e., f_{debr} is $2\times$ larger and smaller when t_{evol} is $2\times$ larger and smaller, respectively, to keep γ the same). There are three important dependencies shown in this figure: (1) the G2 mass fraction is low for both low accretion and high accretion rates, with a peak at $\tilde{R}_{\text{acc}} \sim 0.03$; (2) the G2 mass fraction increases with higher ejection parameter, and (3) the G2 mass fraction depends strongly on the ratio of the gas consumption time to the stellar evolution time.

The first result arises because high \tilde{R}_{acc} causes severe dilution of the p-processed material for later stars that form, and because low \tilde{R}_{acc} causes most of the stars to form quickly and deplete the gas before p-processed elements have time to get into the cloud core. The second result is a consequence of ejecting more early-forming stars than late-forming stars because

of the greater exposure of early-forming stars to time-changing gravitational forces.

The third result indicates the importance of the dimensionless parameter $t_{\text{consume}}/t_{\text{evol}}$. A low value means there are more dynamical times available for stellar ejection before the supernova era begins (at $t = t_{\text{evol}}$), so the first-forming stars become much more depleted compared to the last-forming stars. This increases $M_{\text{G2}}/M_{\text{stars}}$, as shown on the left of Figure 2. It also means there are more massive stars at early times compared to late times, because of the more rapid drop in the star formation rate from faster gas consumption at small t_{consume} . These greater numbers of early massive stars send relatively more p-processed matter into the smaller amount of remaining gas mass in the cloud core, increasing the maximum f_{p} . These trends with lower $t_{\text{consume}}/t_{\text{evol}}$ occur when the density of the cloud core increases, because that lowers the free fall time and, correspondingly, t_{consume} , at a fixed stellar evolution time. Thus we have the important result that *p-process contamination is larger and involves a higher fraction of remaining long-lived stars in a globular cluster when the initial cluster gas density is higher*. This may be the critical clue to the distinct origin of old globular clusters.

Figure 2 suggests that realistic results require a fairly high ejection parameter f_{eject} , on the order of several tenths, which corresponds to a mean time before ejection of low mass stars equal to several tens of dynamical times ($= t_{\text{consume}}/(t_{\text{ff}}f_{\text{eject}})$). Fujii & Portegies Zwart (2013) follow the ejection of stars of various masses from the collapsed core of a cluster owing to binary star interactions. The number of ejected high mass stars per cluster is fairly low, although it can account well enough for runaway OB stars in the field. The number of ejected low mass stars, which are of greatest interest in the present context, is much higher, following the stellar IMF (see their figure 1). They did not do a simulation that is exactly what we need, which would involve a lowest stellar mass less than $0.1 M_{\odot}$ and a cluster more massive than $10^6 M_{\odot}$. In their most relevant case, which had the lowest mass stars, the fraction of stars ejected was 0.4%. That is only for the binary star mechanism, however. Here we envision a much more dynamic environment in which gaseous mass motions from multi-star interactions and winds stochastically change the whole cluster core potential, as in simulations of dwarf galaxy nuclei (El-Badry et al. 2016). That second process, in addition to the possible presence of several dense cores in a proto-GC, each of which has one or more important massive binaries for stellar ejection, could possibly bring the ejection fraction per dynamical time up to the required value.

The dependence of relative G2 mass and processed fraction, f_{p} , on t_{consume} is shown in Figure 3, where we assume fixed f_{debr} , f_{HM} , f_{eject} , and t_{evol} and vary only t_{consume} . In this case the input parameters are dimensional, with t_{consume} up to ~ 1.4 Myr and $R_{\text{acc}} = 0$ (blue curves) and $4 \times 10^5 M_{\odot} \text{ Myr}^{-1}$ (red curves). There are sharp decreases in the relative

mass of the second generation (left panel) and the maximum processed fraction (right panel) as the consumption time increases, which corresponds to a decrease in cloud core density. Because the bulk peculiarity of old GCs is in these two quantities, it seems evident that *the primary distinction between clusters that formed in the early universe and most of the main-disk clusters forming today is cloud-core density.*

4. Conclusions

We present a model of star formation in massive dense clusters that may be relevant to the formation of old globular clusters. This model has several key features that should cause a cluster to form stars with a wide range of p-processed elements, in agreement with observations. These features are:

- A $10^6 - 10^7 M_{\odot}$ cloud core with a density of $\sim 10^6 \text{ cm}^{-3}$, giving a free fall time of $\sim 0.03 \text{ Myr}$. The corresponding virial velocity is $\sim 80 \text{ km s}^{-1}$, which is comparable to the turbulent speed in an L^* galaxy at the same redshift where the GC forms. Such a core is tightly bound and should form stars with an elevated star formation efficiency per unit free fall time, assumed here to be $\sim 10\%$. The free fall time and efficiency combine to give a gas consumption time that is much shorter than the evolution time of a high mass star. Then many generations of stars form in the gaseous debris of earlier generations.
- Interactions between massive stars at close range, including massive binary star interactions with single stars and massive stellar mergers, which lead to the swelling and dispersal of massive stellar envelopes and the dispersal of extruded equatorial disks around rapidly rotating massive stars. The dispersed envelope gas carries p-processed elements into the cloud core where it gets incorporated into new stars.
- Rapid stellar ejection driven by the time-changing gravitational potential of multi-star interactions and pressurized gas motions. The ejection rate is assumed to scale with the dynamical rate in the cluster. We point out that stars ejected from a cluster with a terminal velocity equal to only several tenths of the cloud core virial speed can move through the host galaxy at greater than the galaxy's escape speed and thereby leave the host altogether. Such stellar loss may solve the problem of missing halo stars in Fornax and WLM, which have very low escape speeds.
- Star formation in the cloud core using gas that is a combination of original core gas, stellar debris that becomes more and more contaminated by p-processed elements over

time, and newly accreted gas with the original abundances. Because the consumption time at high density is much less than the lifetime of a massive star, many generations of stars form before supernovae finally clear the gas away. We assume that each generation has a complete and normal IMF. We track the high mass stars for the production of p-processed elements, and the low mass stars for comparison to GCs today.

As a result of these assumptions, we produce GC stellar populations with approximately the observed range, mass, and radial distributions of p-process contamination. We find that the mass fraction of the final GC in the form of contaminated stars (i.e., the “2nd generation” fraction), and the maximum amount of p-process contamination in the late-forming stars, both increase strongly with cloud core density. This result suggests that the primary difference between old GCs with their significant amounts of p-process contamination and young super-massive star clusters that show little evidence for self-enrichment is that the cluster-forming clouds at high redshift have higher densities. This is to be expected because high redshift galaxies have larger gas fractions, higher gas surface densities and faster turbulent speeds than all but the most active galaxies today. As a result, the pressures in high-redshift galaxies are high, and the densities in the star-forming cloud cores should be high too.

This paper benefited from interesting discussions with Dr. Stefanie Walch at an early stage of this investigation, and from comments by the referee.

REFERENCES

- Bally, J., & Zinnecker, H. 2005, *AJ*, 129, 2281
- Bastian, N., Lamers, H. J. G. L. M., de Mink, S.E., Longmore, S.N., Goodwin, S. P., & Gieles, M. 2013, *MNRAS*, 436, 2398
- Bastian, N. Cabrera-Ziri, I., Davies, B., & Larsen, S.S. 2013, *MNRAS*, 436, 2852
- Bastian N. & Strader J., 2014, *MNRAS*, 443, 3594
- Bastian, N., Hollyhead, K., & Cabrera-Ziri, I. 2014, *MNRAS*, 445, 378
- Bastian, N. 2015, in *IAUS 316*, arXiv.1510.01330
- Bate, M.R., & Bonnell, I.A. 2005, *MNRAS*, 356, 1201
- Bekki, K., & Tsujimoto, T. 2016, *ApJ*, 831, 70

- Bonifacio, P., Pasquini, L., Molaro, P., et al. 2007, *A&A*, 470, 153
- Cabrera-Ziri I., Bastian N., Davies B., Magris G., Bruzual G., Schweizer F., 2014, *MNRAS*, 441, 2754
- Cabrera-Ziri, I., Niederhofer, F., Bastian, N., et al. 2016, *MNRAS*, 459, 4218
- Carretta E. 2006, *AJ*, 131, 1766
- Carretta, E., Bragaglia, A., Gratton, R. G., Lucatello, S., & D’Orazi, V. 2012, *ApJL*, 750, L14
- Carretta E., 2014, *ApJ*, 795, L28
- Carretta, E., Bragaglia, A., Gratton, R. G., D’Orazi, V., Lucatello, S., Momany, Y., Sollima, A., Bellazzini, M., Catanzaro, G., & Leone, F. 2014, *A&A*, 564A, 60
- Charbonnel, C. 2005, in *IAU Symp.*, 228, ed. Hill, V. Francois, P., & Primas, F., pp.347
- Cottrell, P. L., & Da Costa, G. S. 1981, *ApJ*, 245, L79
- Crowther, P. A., Schnurr, O., Hirschi, R., et al. 2010, *MNRAS*, 408, 731
- Crowther, P. A., Caballero-Nieves, S. M., Bostroem, K. A., et al. 2016, *MNRAS*, 458, 624
- Daddi, E., Bournaud, F., Walter, F., et al. 2010, *ApJ*, 713, 686
- Decressin, T., Meynet, G., Charbonnel, C., Prantzos, N., & Ekström, S. 2007, *A&A*, 464, 1029
- Decressin T., Charbonnel C., & Meynet G. 2007b, *A&A*, 475, 859
- de Mink S. E., Pols O. R., Langer N., & Izzard R.G., 2009, *A&A*, 507, L1
- Denissenkov, P. A., & Denissenkova, S. N. 1990, *Sov. A Lett.*, 16, 275
- Denissenkov, P. A., & Hartwick, F. D. A. 2014, *MNRAS*, 437, 21
- Denissenkov, P. A., VandenBerg, D. A., Hartwick, F. D. A., et al. 2015, *MNRAS*, 448, 3314
- D’Ercole A., Vesperini E., D’Antona F., McMillan S.L.W., & Recchi S., 2008, *MNRAS*, 391, 825
- D’Ercole, A., D’Antona, F., & Vesperini, E. 2016, *MNRAS*, 461, 4088
- Dickens, R. J., Croke, B. F. W., Cannon, R.D., & Bell, R. A. 1991, *Nature*, 351, 212

- Ebisuzaki, T., Makino, J., Tsuru, T., Go., Funato, Y., Portegies Zwart, S., Hut, P., McMillan, S., Matsushita, S., Matsumoto, H., & Kawabe, R. 2001, *ApJ*, 562, L19
- El-Badry, K., Wetzel, A., Geha, M., Hopkins, P., Kereš, D., Chan, T., & Faucher-Giguère, C.-A. 2016, *ApJ*, 820, 131
- Elmegreen, B.G., Malhotra, S., Rhoads, J. *ApJ*, 757, 9
- Förster Schreiber, N. M., Genzel, R., Bouché, N., et al. 2009, *ApJ*, 706, 1364
- Fregeau, J. M., Cheung, P., Portegies Zwart, S. F., Rasio, F. A. 2004, *MNRAS*, 352, 1
- Fujii, M. S., & Portegies Zwart, S. 2013, *MNRAS*, 430, 1018
- Gaburov, E., Lombardi, J.C., Jr., & Portegies Zwart, S. 2010, *MNRAS*, 402, 105
- Genzel, R., Tacconi, L. J., Gracia-Carpio, J., et al. 2010, *MNRAS*, 407, 2091
- Gieles, M. & Renaud, F. 2016, *MNRAS*, 463, L103
- Ginsburg, A., Goss, W. M., Goddi, C., et al. 2016, *A&A*, 595A, 27
- Governato, F., Zolotov, A., Pontzen, A., Christensen, C., Oh, S. H., Brooks, A. M., Quinn, T., Shen, S., & Wadsley, J. 2012, *MNRAS*, 422, 1231
- Gratton R. G., Sneden C., Carretta E., & Bragaglia A. 2000, *A&A*, 354, 169
- Gratton, R., Bonifacio, P., Bragaglia, A., et al. 2001, *A&A*, 369, 87
- Gratton, R., Sneden, C., & Carretta, E. 2004, *ARA&A*, 42, 385
- Gratton, R.G., Carretta, E., Bragaglia, A. 2012, *A&A Rev.*, 20, 50
- Harris, W. E. & Racine, R. 1979, *ARA&A*, 17, 241
- Heger A., Fryer C. L., Woosley S. E., Langer N., Hartmann D. H., 2003, *ApJ*, 591, 288
- Herrera, C. N., Boulanger, F., Nesvadba, N.P.H., & Falgarone, E. 2012, *A&A*, 538, L9
- Hopkins, P.F., Murray, N., Quataert, E., Thompson, T.A. 2010, *MNRAS*, 401, L19
- Johnson, K. E., Leroy, A. K., Indebetouw, R., Brogan, C.L., Whitmore, B.C., Hibbard, J., Sheth, K., & Evans, A. S. 2015, *ApJ*, 806, 35
- Khalaj, P., & Baumgardt, H. 2016, *MNRAS*, 457, 479

- Klessen, R.S., Burkert, A., Bate, M.R. 1998, *ApJ*, 501, L205
- Krause, M.G.H., Charbonnel, C., Bastian, N., & Diehl, R. 2016, *A&A*, 587A, 53
- Krumholz, M.R. & Tan, J.C. 2007, *ApJ*, 654, 304
- Langer, G. E., Hoffman, R., & Sneden, C. 1993, *PASP*, 105, 301
- Larsen S.S., Brodie J. P., Strader J., 2012, *A&A*, 546, A53
- Larsen S. S., Brodie J. P., Forbes D. A., Strader J., 2014, *A&A*, 565, A98
- Leaman, R., Venn, K.A., Brooks, A.M., Battaglia, G., Cole, A.A., Ibata, R.A., Irwin, M.J.,
McConnachie, A.W., Mendel, J.T., & Tolstoy, E. 2012, *ApJ*, 750, 33
- Li, C., de Grijs, R., Deng, L., Geller, A.M., Xin, Y., Hu, Y., & Faucher-Giguere, C.-A. 2016,
Nature, 529, 502
- Lin, Y., Liu, H.B., Li, D. et al. 2016, *ApJ*, 828, 32
- Marino, A.F., Villanova, S., Milone, A. P., Piotto, G., Lind, K., Geisler, D., & Stetson, P.
B. 2011, *ApJ*, 730, L16
- Martell, S. L., Smolinski, J. P., Beers, T. C., Grebel, E. K. 2011, *A&A*, 534A, 136
- Matzner, C.D., Jumper, P.H. 2015, *ApJ*, 815, 68
- McLaughlin, D.E. & Fall, S. M. 2008, *ApJ*, 679, 1272
- McMillan, S. L. W., Vesperini, E., & Portegies Zwart, S. F. 2007, *ApJL*, 655, L45
- Myers P. C. 2009, *ApJ*, 700, 1609
- Ostriker, Eve C. 1999, *ApJ*, 513, 252
- Paresce, F. & De Marchi, G. 2000, *ApJ*, 534, 870
- Pasquini, L., Bonifacio, P., Molaro, P., et al. 2005, *A&A*, 441, 549
- Prantzos, N., & Charbonnel, C. 2006, *A&A*, 458, 135
- Reipurth B. & Clarke C. 2001, *AJ*, 122, 432.
- Renzini A., 2013, *Mem. Soc. Astron. Ital.*, 84, 162
- Renzini, A., D’Antona, F., Cassisi, S. et al. 2015, *MNRAS*, 454, 4197

- Simpson, J.D., Martell, S.L., Navin, C.A. 2017, MNRAS, 465, 1123
- Smith, L. J., Crowther, P. A., Calzetti, D., Sidoli, F. 2016, ApJ, 823, 38
- Tacconi, L. J., Genzel, R., Neri, R. et al. 2010, Nature, 463, 781
- Umbreit, S., Chatterjee, S., Rasio, F.A. 2008, ApJ, 680, L113
- Walker, M.G., Mateo, M., Olszewski, E.W., Bernstein, R., Wang, X., & Woodroffe, M. 2006, AJ, 131, 2114
- Walker, D. L., Longmore, S. N., Bastian, N., Kruijssen, J. M. D., Rathborne, J. M., Galvn-Madrid, R., & Liu, H. B. 2016, MNRAS, 457, 4536
- Wunsch, R., Palous, J., Tenorio-Tagle, G., Munoz-Tunon, C., & Ehlerova, S. 2015, IAU General Assembly, Meeting 29, id.2254808
- Yong D., Grundahl F., Norris J. E., 2014, MNRAS, 13, 3319

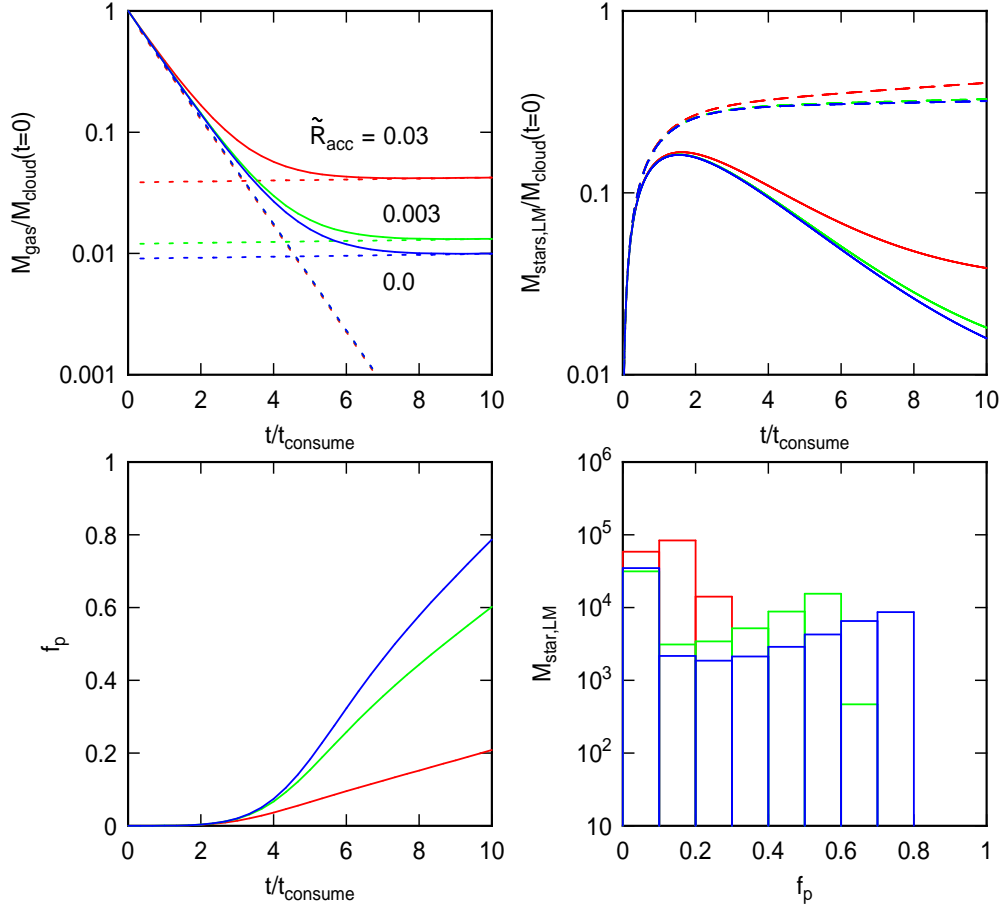


Fig. 1.— Models for the formation of globular clusters with three different normalized accretion rates onto the cloud core. The top-left panel shows the relative core gas mass as a function of time, in units of the gas consumption time. The dotted lines are the separate exponential solutions from equation (17), whose sum equals the total solution. The core mass decreases faster when there is no accretion. The top right panel shows the mass in low mass stars for these three cases (designated by the corresponding colors), with dashed lines representing the case when there is no stellar ejection from the cluster, and solid lines showing the case with ejection using an efficiency of $f_{\text{eject}} = 0.4$. The maximum time on the abscissa corresponds to the lifetime of a massive star, since we assume $t_{\text{consume}}/t_{\text{evol}} = 0.1$ for these results. Thus the final mass in low mass stars is about one-tenth of the total formed mass in stars of this type. The lower left panel shows the time-increase in the processed fraction of gas in the cloud core, defined as the ratio of the p-processed mass to the current core gas mass. The processed fraction increases with time as massive stars evolve, and it is higher when the accretion rate is low because then there is less dilution of stellar envelope material with pristine gas. The lower right panel shows the distribution of processed fraction among the low mass stars at the end of the star formation, when $t/t_{\text{consume}} = 10$. There is a continuum of f_p because stars form continuously as the core gas is contaminated. We consider the first generation stars to be those in the lowest bin. The numbers of these stars is relatively large in all cases, but the cumulative number in bins of higher f_p can be larger.

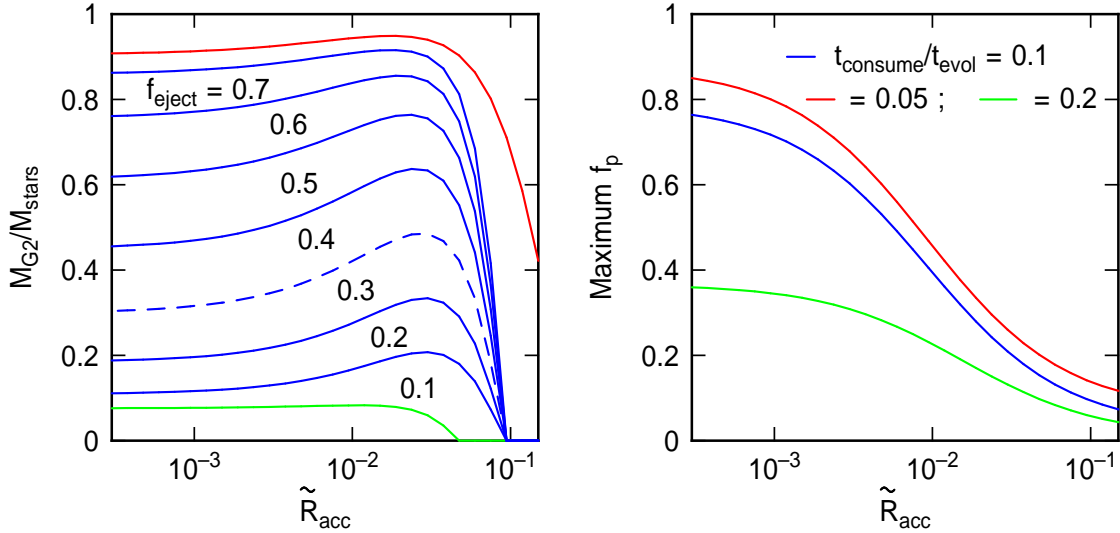


Fig. 2.— (Left) The fraction of low mass stars in the “2nd generation,” defined to be those in all but the lowest bin of f_p from figure 1. This fraction is shown as a function of the normalized accretion rate onto the cloud core, and for different values of the efficiency of stellar ejection from the cluster, f_{eject} . The G2 fraction is low at low \tilde{R}_{acc} because then star formation ends quickly and there is too little time for p-processed elements to get into the gas for subsequent generations of star formation. This fraction is low also at high \tilde{R}_{acc} because then the core is highly diluted with accreted pristine gas. It peaks at around $\tilde{R}_{acc} \sim 0.3$, which is when the accretion rate is 0.3 times the initial core mass divided by the gas consumption time. Higher f_{eject} produces higher G2 fractions because then a higher proportion of early-forming low-mass stars, which have near-G1 abundances, have been ejected. (Right) The maximum value of the processed fraction, f_p , is shown versus the normalized accretion rate for three different cases of the relative consumption time. The low and high cases are also shown in the left-hand panel using the same colors. The curves in the right-hand panel are independent of f_{eject} , which only affects the proportion of stars at various f_p , but not the maximum in f_p . The result indicates that G2 stars reach a higher p-processed fraction if the accretion rate is low, because then the dilution of stellar debris by pristine gas is smaller.

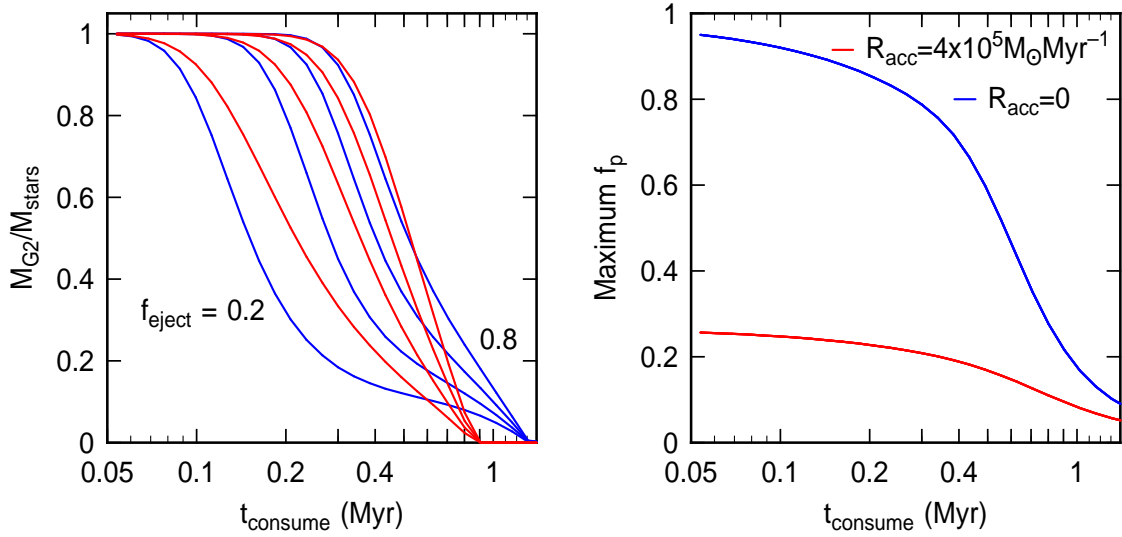


Fig. 3.— The effect is shown of the star formation consumption time on the G2 mass fraction (left) and the maximum processed fraction (right). Longer consumption times correspond to slower star formation and less production of p-processed gas before the supernova era begins. They also correspond to less stellar ejection from the cluster, which should operate on the dynamical time (proportional to the consumption time) and therefore to a greater residual of G1 stars, also lowering the G2 fraction.